

1 **Whole genome analysis illustrates global clonal population structure of the**
2 **ubiquitous dermatophyte pathogen *Trichophyton rubrum***

3
4 Gabriela F. Persinoti^{*,§§§§}, Diego A. Martinez^{†,§§§§,1}, Wenjun Li^{‡,§§§§,2}, Aylin Döğen^{‡,§}, R.
5 Blake Billmyre^{‡,3}, Anna Averette[‡], Jonathan M. Goldberg^{†,4}, Terrance Shea[†], Sarah
6 Young[†], Qiandong Zeng^{†,5}, Brian G. Oliver^{**}, Richard Barton^{††}, Banu Metin^{‡‡}, Süleyha
7 Hilmioğlu-Polat^{§§}, Macit Ilkit^{***}, Yvonne Gräser^{†††}, Nilce M. Martinez-Rossi^{*}, Theodore C.
8 White^{‡‡‡}, Joseph Heitman^{‡,****}, Christina A. Cuomo^{†,****}

9
10 ^{*}Department of Genetics, Ribeirão Preto Medical School, University of São Paulo, Brazil

11 [†]Broad Institute of MIT and Harvard, Cambridge, Massachusetts 02142, USA

12 [‡]Department of Molecular Genetics and Microbiology, Duke University Medical Center, Durham,
13 North Carolina, USA

14 [§]Department of Pharmaceutical Microbiology, Faculty of Pharmacy, University of Mersin, Mersin,
15 Turkey

16 ^{**}Center for Infectious Disease Research, Seattle, Washington, USA

17 ^{††}University of Leeds, Leeds, United Kingdom

18 ^{‡‡}Department of Food Engineering, Faculty of Engineering and Natural Sciences, Istanbul
19 Sabahattin Zaim University, Istanbul, Turkey

20 ^{§§}Department of Microbiology, Faculty of Medicine, University of Ege, Izmir, Turkey

21 ^{***}Division of Mycology, Department of Microbiology, Faculty of Medicine University of Çukurova,
22 Adana, Turkey

23 ^{†††}Institute of Microbiology and Hygiene, University Medicine Berlin - Charité, Berlin, Germany

24 ^{‡‡‡}School of Biological Sciences, University of Missouri-Kansas City, Kansas City, Missouri, USA

25 ^{§§§§}equal contribution as first authors. ^{****} corresponding authors.

26 Current addresses: ¹Veritas Genetics, Danvers, Massachusetts 01923, USA; ²National Center
27 for Biotechnology Information (NCBI), 8600 Rockville Pike, Bethesda, MD 20894, USA;

28 ³Stowers Institute for Medical Research, Kansas City, Missouri, USA; ⁴Harvard T. H. Chan
29 School of Public Health, Boston, Massachusetts 02115, USA; ⁵LabCorp, Westborough, MA
30 01581, USA.

31

32 Data access: Genome sequence data is available in NCBI under the Umbrella BioProject
33 PRJNA186851.

34

35 **Running title:** Global clonal population structure of *Trichophyton rubrum*

36

37 **Keywords:** *Trichophyton rubrum*, *Trichophyton interdigitale*, dermatophyte, genome
38 sequence, MLST, mating, recombination, LysM

39

40 **Corresponding authors:**

41 Christina A. Cuomo, Broad Institute, 415 Main Street, Cambridge, MA 02142. Phone:
42 (617) 714-7904. Email: cuomo@broadinstitute.org

43

44 Joseph Heitman, 322 CARL Building, Box 3546, Duke University Medical Center,
45 Durham, N.C. 27710. Phone: (919) 684-2824. Email: heitm001@duke.edu

46 **Abstract**

47 Dermatophytes include fungal species that infect humans, as well as those which also
48 infect other animals or only grow in the environment. The dermatophyte species
49 *Trichophyton rubrum* is a frequent cause of skin infection in immunocompetent
50 individuals. While members of the *T. rubrum* species complex have been further
51 categorized based on various morphologies, the population structure and ability to
52 undergo sexual reproduction are not well understood. In this study, we analyze a large
53 set of *T. rubrum* and *Trichophyton interdigitale* isolates to examine mating types,
54 evidence of mating, and genetic variation. We find that nearly all isolates of *T. rubrum*
55 are of a single mating type, and that incubation with *T. rubrum* morphotype *megrinii*
56 isolates of the other mating type failed to induce sexual development. While the region
57 around the mating type locus is characterized by a higher frequency of SNPs compared
58 to other genomic regions, we find that the population is remarkably clonal, with highly
59 conserved gene content, low levels of variation, and little evidence of recombination.
60 These results support a model of recent transition to asexual growth when this species
61 specialized to growth on human hosts.

63 **Introduction**

64 Dermatophyte species are the most common fungal species causing skin infections. Of
65 the more than 40 different species infecting humans, *Trichophyton rubrum*, the major
66 cause of athlete's foot, is the most frequently observed (Achterman and White 2013;
67 White *et al.* 2014). Other species are more often found on other skin sites, such as
68 those found on the head, including *Trichophyton tonsurans* and *Microsporum canis*.
69 Some dermatophyte species only cause human infections, including *T. rubrum*, *T.*
70 *tonsurans*, and *T. interdigitale*. Other species, including *Trichophyton benhamiae*,
71 *Trichophyton equinum*, *Trichophyton verrucosum*, and *M. canis*, infect mainly animals
72 and occasionally humans, while others such as *Microsporum gypseum* (*Nannizzia*
73 *gypsea* (de Hoog *et al.* 2017a)) are commonly found in soil and rarely infect animals. In
74 addition to the genera *Trichophyton* and *Microsporum*, *Epidermophyton* and *Nannizzia*
75 are other genera of dermatophytes that commonly cause infections in humans (de Hoog
76 *et al.* 2017b). The species within these genera are closely related phylogenetically and

77 are within the Ascomycete order Onygenales, family Arthrodermataceae (White *et al.*
78 2008; de Hoog *et al.* 2017a).

79
80 The *Trichophyton rubrum* species complex includes several “morphotypes,” many of
81 which rarely cause disease, and *T. violaceum*, a species that causes scalp infections
82 (Gräser *et al.* 2000; de Hoog *et al.* 2017a). Some morphotypes display phenotypic
83 variation, though these differences can be modest. For example, *T. rubrum* morphotype
84 *raubitscheckii* differs from *T. rubrum* in production of urease and in colony pigmentation
85 and colony appearance under some conditions (Kane *et al.*). *T. rubrum* morphotype
86 *megrinii*, which is commonly isolated in Mediterranean countries, requires L-histidine for
87 growth unlike other *T. rubrum* isolates (Gräser *et al.* 2000). However, little variation has
88 been observed between these and other morphotypes in the sequence of individual loci,
89 such as the ITS rDNA locus; additionally, some of the morphotypes do not appear to be
90 monophyletic (Gräser *et al.* 2000, 2007; de Hoog *et al.* 2017a), complicating any simple
91 designation of all types as separate species. Combining morphological and multilocus
92 sequence typing (MLST) data has helped clarify relationships of the major genera of
93 dermatophytes and resolved polyphyletic genera initially assigned by morphological or
94 phenotypic data.

95
96 Mating has been observed in some dermatophyte species, although not to date in strict
97 anthropophiles including *T. rubrum* (Metin and Heitman 2017). Mating type in
98 dermatophytes, as in other Ascomycetes, is specified by the presence of one of two
99 idiomorphs at a single mating type (*MAT*) locus; each idiomorph includes either an
100 alpha box domain or HMG domain transcription factor gene (Li *et al.* 2010). In the
101 geophilic species *M. gypseum*, isolates of opposite mating type (*MAT1-1* and *MAT1-2*)
102 undergo mating and produce recombinant progeny (Li *et al.* 2010). In the zoophilic
103 species *T. benhamiae*, both mating types are detected in the population and mating
104 assays produced fertile cleistothecia (Symoens *et al.* 2013), structures that contain
105 meiotic ascospores. In a study examining 600 isolates of *T. rubrum*, only five appeared
106 to produce structures similar to cleistothecia (Young 1968), suggesting inefficient
107 development of the spores required for mating. Sexual reproduction experiments of *T.*

108 *rubrum* with tester strains of *Trichophyton simii*, a skin infecting species that is closely
109 related to *T. mentagrophytes*, have been reported and one recombinant isolate was
110 characterized, consistent with a low frequency of mating of *T. rubrum* (Anzawa *et al.*
111 2010). Further, sexual reproduction of *T. rubrum* may be rare in natural populations, as
112 a single mating type (*MAT1-1*) has been noted in Japanese isolates (Kano *et al.* 2013),
113 matching that described in the *T. rubrum* reference genome of CBS 118892 (Li *et al.*
114 2010).

115
116 Here we describe genome-wide patterns of variation in *T. rubrum*, revealing a largely
117 clonal population. This builds on prior work to produce reference genomes for *T. rubrum*
118 (Martinez *et al.* 2012) and other dermatophytes (Burmester *et al.* 2011; Martinez *et al.*
119 2012). Genomic analysis of two divergent morphotypes of *T. rubrum*, *megrinii* and
120 *soudanense*, reveal hotspots of variation linked to the mating type locus suggestive of
121 recent recombination. While nearly all *T. rubrum* isolates are of a single mating type
122 (*MAT1-1*), the sequenced *megrinii* morphotype isolate contains a *MAT1-2* locus,
123 suggesting the capacity for infrequent mating in the population. Additionally, we
124 examine variation in gene content across dermatophyte genomes including the first
125 representatives of *T. interdigitale*.

126

127 **Materials and methods**

128 **Isolate selection, growth conditions, and DNA isolation**

129 Isolates analyzed are listed in **Table S1**, including the geographic origin, site of origin,
130 and mating type for each. Isolates selected for whole genome sequencing were chosen
131 to maximize diversity by covering the main known groups. For whole genome
132 sequencing, 10 *T. rubrum* isolates and 2 *T. interdigitale* isolates were selected,
133 including representatives of the major morphotypes of *T. rubrum* (**Table S2**). Growth
134 and DNA isolation for whole genome sequencing were performed as previously
135 described (Martinez *et al.* 2012).

136

137 For MLST analysis, a total of 80 *T. rubrum* isolates and 11 *T. interdigitale* isolates were
138 selected for targeted sequencing. Isolates were first grown on PDA medium (Difco) for

139 10 days at 25°C. Genomic DNA was extracted using an Epicentre Masterpure Yeast
140 DNA purification kit (catalog number MPY08200). Fungal isolates were harvested from
141 solid medium using sterile cotton swabs, transferred to microcentrifuge tubes, and
142 washed with sterile PBS. Glass beads (2 mm) and 300 µL yeast cell lysis solution
143 (Epicentre) were added to the tube to break down fungal cells, and the protocol
144 provided by Epicentre was then followed. The contents of the tube were mixed by
145 vortexing and incubated at 65°C for 30 minutes, followed by addition of 150 µl Epicentre
146 MPC Protein Precipitation Solution. After vortexing, the mixture was centrifuged for 10
147 minutes, followed by isopropanol precipitation and washing with 70% ethanol. The DNA
148 pellet was dissolved in TE buffer.

149

150 For mating assays, we investigated 55 *T. rubrum* and 9 *T. interdigitale* isolates
151 recovered from Adana and Izmir, Turkey. *T. simii* isolates CBS 417.65 MT -, CBS
152 448.65 MT + and morphotype *megninii* isolates CBS 389.58, CBS 384.64, and CBS
153 417.52 were also used in mating assays. DNA extraction was performed according to
154 the protocol described by Turin et al. (Turin et al. 2000). These isolates were typed by
155 ITS sequence analysis. rDNA sequences spanning the internal transcribed spacer (ITS)
156 1 region were PCR-amplified using the universal fungal primers ITS1 (5'-
157 TCCGTAGGTGAACCTGCGG3') and ITS4 (5'-CCTCCGCTTATTGATATGC-3') and
158 sequenced on an ABI PRISM 3130XL genetic analyzer at Refgen Biotechnologies using
159 the same primers (Ankara, Turkey). CAP contig assembly software, included in the
160 BioEdit Sequence Alignment Editor 7.0.9.0 software package, was used to edit the
161 sequences (Hall 1999). Assembled DNA sequences were characterized using BLAST in
162 GenBank.

163

164 **Multilocus sequence typing (MLST)**

165 A total of 108 isolates were subjected to MLST analysis (**Table S3**). For each isolate,
166 three loci (the *TruMDR1* ABC transporter (Cervellati et al. 2006), an intergenic region
167 (IR), and an alpha-1,3-mannosyltransferase (CAP59 protein domain)), with high
168 sequence diversity between *T. rubrum* CBS 118892 (GenBank accession:
169 NZ_ACPH00000000) and *T. tonsurans* CBS 112818 (GenBank accession:

170 ACPI00000000), were selected as molecular markers in MLST. The following conditions
171 were used in the PCR amplification of the three loci: an initial 2 min of denaturation at
172 98°C, followed by 35 cycles of denaturation for 10 sec at 98°C, an annealing time of 15
173 sec at 54°C, and an extension cycle for 1 min at 72°C. The amplification was completed
174 with an extension period of 5 min at 72°C. PCR amplicons were sequenced using the
175 same PCR primers on an ABI PRISM 3130XL genetic analyzer by Genewiz, Inc. (**Table**
176 **S4**). Electropherograms of Sanger sequencing were examined and assembled using
177 Sequencher 4.8 (Gene Codes). Alternatively, sequences were obtained from genome
178 assemblies (**Table S5**).

179
180 To confirm the species typing for four isolates (MR857, MR827, MR816, and MR897),
181 the ITS1, 5.8S, and ITS2 region was amplified using the ITS5 (5'-
182 GAAGTAAAAGTCGTAACAAGG-3') and Mas266 (5'-
183 GCATTCCCAAACAACACTCGACTC-3') primers with initial denaturation at 94°C for 4
184 minutes, 35 cycles of denaturation at 94°C for 30 seconds, annealing at 60°C for 30
185 seconds, extension at 72°C for 1 minute, and final extension at 72°C for 10 minutes.
186 The reactions were carried out using a BioRad C1000 Touch thermocycler. ABI
187 sequencing reads were compared to the dermatophyte database of the Westerdijk
188 Fungal Biodiversity Institute. The sequences of MR857 and MR827 isolates were 99.6%
189 identical to that of the isolate RV 30000 of the African race of *T. benhamiae* (GenBank
190 AF170456).

191 192 **Mating type determination**

193 To identify the mating type of each isolate, primers were designed to amplify either the
194 alpha or HMG domain of *T. rubrum* (**Table S6**). For most isolates, PCR amplification
195 was performed using an Eppendorf epGradient Mastercycler, and reactions were
196 carried out using the following conditions for amplification: initial denaturation at 94°C
197 for 4 minutes, 35 cycles of denaturation at 94°C for 30 seconds, annealing at 55°C for
198 30 seconds, extension at 72°C for 1 minute, with a final extension at 72°C for 7 minutes.
199 For isolates from Turkey, PCR amplifications were performed with the same primers
200 using a Biorad C1000 Touch™ Thermal Cycler, and slightly modified conditions were

201 used for amplification: initial denaturation at 94°C for 5 minutes, 35 cycles of
202 denaturation at 95°C for 45 seconds, annealing at 55°C for 1.5 minutes, and extension
203 at 72°C for 1 minute, and final extension at 72°C for 10 minutes. The presence of the
204 alpha box gene, which is indicative of the *MAT1-1* mating type, or the HMG domain,
205 which is indicative of the *MAT1-2* mating type, was identified using primers
206 JOHE21771/WL and JOHE21772/WL, creating a 500-bp product, and JOHE21773/WL
207 and JOHE21774/WL, creating a 673-bp product, respectively. *Trichophyton rubrum* MR
208 851 was used as a positive control for *MAT1-1*, and morphotype *megninii* CBS 389.58,
209 CBS 384.64, CBS 417.52, and *T. interdigitale* MR 8801 were used as positive controls
210 for *MAT1-2*. The mating type was assigned based on the presence or absence of PCR
211 products on 1.5% agarose gels. For the whole genome sequenced isolates, mating type
212 was determined by analysis of assembled and annotated genes.

213

214 **Mating assays**

215 Mating assays were performed using both Medium E (12 g/L oatmeal agar (Difco), 1 g/L
216 MgSO₄·7H₂O, 1 g/L NaOH₃, 1g/L KH₂PO₄, and 16 g/L agar (Weitzman and Silva-Hutner
217 1967)) and Takashio medium (1/10 Sabouraud containing 0.1% neopeptone, 0.2%
218 dextrose, 0.1% MgSO₄·7H₂O, and 0.1%. KH₂PO₄). *MAT1-1* and *MAT1-2* isolates grown
219 on Sabouraud Dextrose Agar (SDA) for one week were used to inoculate both Medium
220 E and Takashio medium plates pairwise 1 cm apart from each other. The plates were
221 incubated at room temperature without Parafilm in the dark for 4 weeks. The petri
222 dishes were examined under light microscopy for sexual structures.

223

224 **Genome sequencing, assembly, and annotation**

225 For genome sequencing, we constructed a 180-base fragment library from each
226 sample, by shearing 100 ng of genomic DNA to a median size of ~250 bp using a
227 Covaris LE instrument and preparing the resulting fragments for sequencing as
228 previously described (Fisher *et al.* 2011). Each library was sequenced each on the
229 Illumina HiSeq 2000 platform. Roughly 100X of 101 base-paired Illumina reads were
230 assembled using ALLPATHS-LG (Gnerre *et al.* 2011) run with assisting mode utilizing
231 *T. rubrum* CBS118892 as a reference. For most genomes, assisting mode 2 was used

232 (ASSISTED_PATCHING=2) with version R42874; for *T. interdigitale* H6 and *T. rubrum*
233 MR1463 version R44224 was used. For *T. rubrum* morphotype *megninii* CBS 735.88
234 and *T. rubrum* morphotype *raubitschekii* CBS 202.88 mode 2.1 was used
235 (ASSISTED_PATCHING=2.1) with version R47300. Assemblies were evaluated using
236 GAEMR (<http://software.broadinstitute.org/software/gaemr/>); contigs corresponding to
237 the mitochondrial genome or contaminating sequence from other species were removed
238 from assemblies.

239

240 The *Trichophyton* assemblies were annotated using a combination of expression data,
241 conservation information, and *ab-initio* gene finding methods as previously described
242 (Haas *et al.* 2011). Expression data included Illumina reads (SRX123796) from one
243 RNA-Seq study (Ren *et al.* 2012) and all EST data available in GenBank as of 2012.
244 RNA-Seq reads were assembled into transcripts using Trinity (Grabherr *et al.* 2011).
245 PASA (Haas *et al.* 2003) was used to align the assembled transcripts and ESTs to the
246 genome and identify open reading frames (ORFs); gene structures were also updated in
247 the previously annotated *T. rubrum* CBS118892 assembly (Martinez *et al.* 2012).
248 Conserved loci were identified by comparing the genome with the UniRef90 database
249 (Wu *et al.* 2006) (updated in 2012) using BLAST (Altschul *et al.* 1997). The BLAST
250 alignments were used to generate gene models using Genewise (Birney *et al.* 2004).
251 The *T. rubrum* CBS 118892 genome was aligned with the new genomes using NUCmer
252 (Kurtz *et al.* 2004). These alignments were used to map gene models from *T. rubrum* to
253 conserved loci in the new genomes.

254

255 To predict gene structures, GeneMark, which is self-training, was applied first;
256 GeneMark models matching GeneWise ORF predictions were used to train the other
257 *ab-initio* programs. *Ab-initio* gene-finding methods included GeneMark (Borodovsky *et al.*
258 *al.* 2003), Augustus (Stanke *et al.* 2004), SNAP (Korf 2004) and Glimmer (Majoros *et al.*
259 2004). Next, EVM (Haas *et al.* 2008) was used to select the optimal gene model at each
260 locus. The input for EVM included aligned transcripts from Trinity and ESTs, gene
261 models created by PASA and GeneWise, mapped gene models, and *ab-initio*
262 predictions. Rarely, EVM failed to produce a gene model at a locus likely to encode a

263 gene. If alternative gene models existed at such loci, they were added to the gene set if
264 they encoded proteins longer than 100 amino acids, or if the gene model was validated
265 by the presence of a PFAM domain or expression evidence. Finally, PASA was run
266 again to improve gene-model structure, predict splice variants, and add UTR.

267

268 Gene model predictions in repetitive elements were identified and removed from gene
269 sets if they overlapped TPSI predictions (<http://transposonpsi.sourceforge.net>),
270 contained PFAM domains known to occur in repetitive elements, or had BLAST hits
271 against the Repbase database (Jurka *et al.* 2005). Additional repeats were identified
272 using a BLAT (Kent 2002) self-alignment of the gene set to the genomic sequence
273 (requiring at least 90% nucleotide identity over 100 bases aligned); genes that hit the
274 genome more than eight times using these criteria were removed. Genes with PFAM
275 domains not found in repetitive elements were retained in the gene set, even if they met
276 the above criteria for removing likely repetitive elements from the gene set.

277

278 Lastly, the gene set was inspected to address systematic errors. Gene models were
279 corrected if they contained in-frame stop codons, had coding sequence overlaps with
280 coding regions of other gene models or predicted transfer or ribosomal RNAs, contained
281 exons spanning sequence gaps, had incomplete codons, or with UTRs overlapping the
282 coding sequences of other genes. Transfer RNAs were predicted using tRNAscan
283 (Lowe and Eddy 1997), and ribosomal RNAs were predicted with RNAmmer (Lagesen
284 *et al.* 2007).

285

286 All annotated assemblies and raw sequence reads are available in NCBI (**Table S5**).

287

288 **SNP identification and classification**

289 To identify SNPs within the *T. rubrum* group, Illumina reads for each *T. rubrum* isolate
290 were aligned to the *T. rubrum* CBS 118829 reference assembly using BWA-MEM (Li
291 2013); reads from the H6 *T. interdigitale* were also aligned to the *T. interdigitale* MR 816
292 assembly. The Picard tools (<http://picard.sourceforge.net>) AddOrReplaceReadGroups,
293 MarkDuplicates, CreateSequenceDictionary, and ReorderSam were used to preprocess

294 read alignments. To minimize false positive SNP calls near insertion/deletion (indel)
295 events, poorly aligned regions were identified and realigned using GATK
296 RealignerTargetCreator and IndelRealigner (GATK version 2.7-4 (McKenna *et al.* 2010
297 p. 201)). SNPs were identified using the GATK UnifiedGenotyper (with the haploid
298 genotype likelihood model) run with the SNP genotype likelihood models (GLM). We
299 also ran BaseRecalibrator and PrintReads for base quality score recalibration on sites
300 called using GLM SNP and re-called variants with UnifiedGenotyper emitting all sites.
301 VCFtools (Danecek *et al.* 2011) was used to count SNP frequency in windows across
302 the genome (--SNPdensity 5000) and to measure nucleotide diversity (--site-pi), which
303 was normalized for the assembly size. For comparison, the nucleotide diversity was
304 calculated for the SNPs identified in a set of 159 isolates of *C. neoformans* var. *grubii*, a
305 fungal pathogen that undergoes frequent recombination (Rhodes *et al.* 2017).

306
307 SNPs were mapped to genes using VCFannotator (<http://vcfannotator.sourceforge.net/>),
308 which annotates whether a SNP results in synonymous or non-synonymous change in
309 coding region. The total number of synonymous and non-synonymous sites across the
310 *T. rubrum* CBS 118829 and *T. interdigitale* MR 816 gene sets were calculated across all
311 coding regions using codeml in PAML (version 4.8) (Yang 2007); these totals were used
312 to normalize the ratios of non-synonymous to synonymous SNPs.

313

314 **Copy number variation**

315 To identify regions of *T. rubrum* that exhibit copy number variation between the isolates,
316 we identified windows showing significant variation in normalized read depth using
317 CNVnator (Abyzov *et al.* 2011). The realigned read files used for SNP calling were input
318 to CNVnator version 0.2.5, specifying a window size of 1kb. Regions reported as
319 deletions or duplications were filtered requiring $p\text{-val}1 < 0.01$.

320

321 **Phylogenetic and comparative genomic analysis**

322 To infer the phylogenetic relationship of the sequenced isolates, we identified single
323 copy genes present in all genomes using OrthoMCL (Li *et al.* 2003). Individual orthologs
324 were aligned with MUSCLE (Edgar 2004) and then the alignments were concatenated

325 and input to RAxML (Stamatakis 2006), version 7.3.3 with 1,000 bootstrap replicates
326 and model GTRCAT. RAxML version 7.7.8 was used for phylogenetic analysis of SNP
327 variant in seven *T. rubrum* isolates, with the same GTRCAT model.

328
329 For each gene set, HMMER3 (Eddy 2011) was used to identify PFAM domains using
330 release 27 (Finn *et al.* 2014); significant differences in gene counts for each domain
331 were identified using Fisher's exact test, with p-values corrected for multiple testing
332 (Storey and Tibshirani 2003). Proteins with LysM domains were identified using a
333 revised HMM as previously described (Martinez *et al.* 2012); this HMM includes
334 conserved features of fungal LysM domains including conserved cysteine residues not
335 represented in the PFAM HMM model and identified additional genes with this domain.

336

337 **Construction of paired allele compatibility matrix**

338 To construct SNP profiles, SNPs shared by at least two members of the *T. rubrum*
339 dataset were selected. Private SNPs are not informative for a paired allele compatibility
340 test because they can never produce a positive result. These profiles were then counted
341 across the genome to construct SNP profiles via a custom Perl script. We required
342 profiles to be present at least twice, to minimize the signal from homoplasic mutations.
343 Pairwise tests were then conducted between each of the profiles to look for all four
344 possible allele combinations, which would only occur via either mating or homoplasic
345 mutations.

346

347 **Linkage disequilibrium calculation**

348 Linkage disequilibrium was calculated for *T. rubrum* SNPs in 1kb windows of all
349 scaffolds with VCFtools version 1.14 (Danecek *et al.* 2011), using the --hap-r2 option
350 with a minimum minor allele frequency of 0.2.

351

352 **Data Availability**

353 All genomic data is available in NCBI and can be accessed via the accession numbers
354 in Table S2. The NCBI GenBank accession numbers of the three MLST loci are listed in
355 Table S3.

356
357
358
359
360
361
362
363
364
365
366
367
368
369
370
371
372
373
374
375
376
377

Results

Relationship of global *Trichophyton* isolates using MLST

To examine the relationship of global isolates of *T. rubrum*, we sequenced three loci in each of 104 *Trichophyton* isolates and carried out phylogenetic analysis. The typed isolates included 91 *T. rubrum* isolates, 11 *T. interdigitale* isolates, and 2 *T. benhamiae* isolates (**Table S1**). In addition, data from the genome assemblies of additional dermatophyte species (*T. verrucosum*, *T. tonsurans*, *T. equinum*, and *M. gypseum*) were also included. Three loci — the *TruMDR1* ABC transporter (Cervelatti *et al.* 2006), an intergenic region (IR), and an alpha-1,3-mannosyltransferase (CAP59 protein domain) — were sequenced in each isolate. Phylogenetic analysis of the concatenated loci can resolve species boundaries between the seven species (**Figure 1**). A large branch separates a *T. benhamiae* isolate (MR857) from the previously described genome sequenced isolate (CBS 112371) (**Figure 1**), and the sequences of two loci of a second *T. benhamiae* isolate (MR827) were identical to those of MR857 (**Table S3**). Sequencing of the ITS region of the MR857 and MR827 isolates revealed high sequence similarity to isolates from the *T. benhamiae* African race (**Methods**), which is more closely related to *T. bullosum* than isolates of *T. benhamiae* Americano-European race including CBS112371 (Heidemann *et al.* 2010). Otherwise, the species relationships and groups are consistent between studies.

378 MLST analysis demonstrated that the *T. rubrum* isolates were nearly identical at the
379 three sequenced loci. Remarkably, of the 84 *T. rubrum* isolates sequenced at all three
380 loci, 83 were identical at all positions of the three loci sequenced (genotype 2, **Table**
381 **S3**). Only one isolate, 1279, displayed a single difference at one site in the *TruMDR1*
382 gene (genotype 3, **Table S3**). For the remaining six isolates, sequence at a subset of
383 the loci was generated and matched that of the predominant genotype. Thus, MLST
384 was not sufficient to discern the phylogenetic substructure in the *T. rubrum* population
385 that included six isolates representing different morphotypes (**Table S3**). Similarly, the
386 11 *T. interdigitale* isolates were highly identical at these three loci; two groups were

387 separated by a single nucleotide difference in the IR and the third group contained a 6-
388 base deletion overlapping the same base of the IR (genotypes 1, 5 and 6, **Table S3**).
389 Although most species can be more easily discriminated based on the MLST sequence,
390 *T. equinum* and *T. tonsurans* isolates differed only by a single transition mutation in the
391 IR, which illustrates the remarkable clonality of these species.

392

393 **Genome sequencing and refinement of phylogenetic relationships**

394 As MLST analysis was insufficient to resolve the population substructure of the *T.*
395 *rubrum* species complex, we sequenced the complete genomes of *T. rubrum* isolates
396 representing worldwide geographical origins and five morphotypes: *fischeri*, *kanei*,
397 *megninii*, *raubitschekii*, and *soudanense*. We generated whole genome Illumina
398 sequences for ten *T. rubrum* and two *T. interdigitale* isolates (**Table S2**). The sequence
399 of each isolate was assembled and utilized to predict gene sets. The *T. rubrum*
400 assembly size was very similar across isolates, ranging from 22.5 to 23.2 Mb (**Table**
401 **S5**). The total predicted gene numbers were also similar across the isolates, with
402 between 8,616 and 9,064 predicted genes in the ten *T. rubrum* isolates, and 7,993 and
403 8,116 predicted genes in the two *T. interdigitale* isolates (**Table S5**).

404

405 To infer the phylogenetic relationship of these isolates and other previously sequenced
406 *Trichophyton* isolates, we identified 5,236 single-copy orthologs present in all species
407 and estimated a phylogeny with RAxML (Stamatakis 2006) (**Figure 2A**). This phylogeny
408 more precisely delineates the species groups than that derived from the MLST loci and
409 also illustrates the relationship between the *T. rubrum* isolates (**Figure 2B**). The results
410 of this analysis suggest that the *fischeri* morphotype is not monophyletic, as one *fischeri*
411 isolate (CBS100081) is more closely related to the *raubitschekii* isolate than to the other
412 *fischeri* isolate (CBS 288.86). While a subset of seven *T. rubrum* isolates appear
413 closely related, others show much higher divergence, including the *soudanense* isolate,
414 the *megninii* isolate, the MR1459 isolate, and the CBS 118829 isolate representing the
415 reference genome. The *soudanense* isolate (CBS 452.61) was placed as an outgroup
416 relative to the other *T. rubrum* isolates; this is consistent with this isolate being part of a
417 clade more closely related to *T. violaceum* than to *T. rubrum* (Gräser *et al.* 2000) and

418 with the re-establishment of *soudanense* isolates as a separate species (de Hoog *et al.*
419 2017a).

420
421 To further classify the two *T. interdigitale* isolates, we assembled the ITS region of the
422 ribosomal DNA locus and compared the sequences to previously classified ITS
423 sequences, as *T. interdigitale* isolates differ from *T. mentagrophytes* at the ITS locus
424 (Gräser *et al.* 2008; de Hoog *et al.* 2017a). For the two genomes of these species that
425 we sequenced, MR816 was identical to *T. interdigitale* at the ITS1 locus, whereas the H6
426 isolate appears intermediate between *T. interdigitale* and *T. mentagrophytes*, containing
427 polymorphisms specific to each group (**Figure S1**). Genomic analysis of allele sharing
428 across a wider set of *T. interdigitale* and *T. mentagrophytes* isolates could be used to
429 evaluate the extent of hybrid genotypes and genetic exchange between these two
430 species.

431
432 ***MAT1-1* prevalence and clonality in *T. rubrum***

433 To address if the *T. rubrum* population is capable of sexual reproduction, we surveyed
434 the *MAT* locus of all isolates. Using either gene content in assembled isolates or a PCR
435 assay to assign mating type, we found that 79 of the 80 *T. rubrum* isolates contained
436 the alpha domain gene at the *MAT* locus (*MAT1-1*). In addition, a set of 55 isolates from
437 Turkey were found to harbor the *MAT1-1* allele based on a PCR assay (**Figure S2**).
438 However, the *T. rubrum* morphotype *megninii* isolate contained an HMG gene at the
439 *MAT* locus (*MAT1-2*) (**Figure 3, Table S1**). The presence of both mating types suggests
440 that this species could be capable of mating under some conditions. However the high
441 frequency of a single mating type strongly suggests that *T. rubrum* largely undergoes
442 clonal growth, although other interpretations are also possible (see **Discussion**). In
443 further support of this, a study of 206 *T. rubrum* clinical isolates from Japan noted that
444 all were of the *MAT1-1* mating type (Kano *et al.* 2013).

445
446 A closer comparison of the genome sequences of *T. rubrum* isolates also supports a
447 clonal relationship of this population. Phylogenetic analysis of the seven most closely
448 related *T. rubrum* isolates using SNPs between these isolates (see below) suggests that

449 the isolates have a similar level of divergence from each other (**Figure S3**). This
450 supports that these *MAT1-1 T. rubrum* isolates have likely undergone clonal expansion.

451
452 To test for recombination that could reflect sexual reproduction within the *T. rubrum*
453 population sampled here, we conducted a genome-wide paired allele compatibility test
454 to look for the presence of all four products of meiosis (**Figure 4**). This test is a
455 comparison between two paired polymorphic sites in the population. While the presence
456 of three of the four possible allele combinations at two sites in a population is possible
457 through a single mutation and identity by descent, the presence of all four combinations
458 requires either recombination, or less parsimoniously, a second homoplastic mutation.
459 Four positive tests resulted from this analysis (out of 21 possible), including allele
460 combinations that occurred a minimum of 13 times. This may suggest that
461 recombination is a rare event arising through infrequent sexual recombination occurring
462 in this population although the same mutations and combinations arising via homoplasy
463 (or selection) are difficult to exclude. Based on the number of triallelic sites in the
464 dataset (19), we would predict 9.5 homoplastic sites to have occurred by random
465 chance, which is similar to the number of sites responsible for the positive signals in the
466 compatibility test. In addition, linkage disequilibrium does not decay over increasing
467 distance between SNPs in *T. rubrum* (**Figure S4**), which further supports a low level of
468 recombination in this species; sequencing additional diverse isolates would help to
469 address if some isolates or lineages were more prone to recombination.

470
471 We also characterized the *MAT* locus of the newly sequenced *T. interdigitale* isolates
472 (H6 and MR816) and found that both contain an HMG domain gene. These *T.*
473 *interdigitale* isolates were more closely related to *T. equinum* (*MAT1-2*) and *T.*
474 *tonsurans* (*MAT1-1*) than *T. rubrum* (**Figure 2A**). To survey the mating type across a
475 larger set of *T. interdigitale* isolates, a set of 11 additional isolates from Turkey were
476 typed. Based on PCR analysis, all *T. interdigitale* isolates harbor the *MAT1-2* allele
477 (**Figure S2**).

478

479 The mating abilities of the isolates were tested by conducting mating assays with
480 potentially compatible isolates of *T. rubrum*, including the *megninii* morphotype, *T.*
481 *interdigitale*, and *T. simii* (**Table S7**). These experiments were conducted using both
482 Takashio and E medium at room temperature (approximately 21 to 22°C) without
483 Parafilm in the dark. Although the assay plates were incubated for longer than five
484 months, ascomata or ascomatal initials were not observed (**Figure S5**). While it is
485 possible that mating may occur under cryptic conditions (Heitman 2010), this data
486 suggests that the conditions tested are not sufficient for the initiation of mating
487 structures in *T. rubrum*.

488

489 **Genome-wide variation patterns in *T. rubrum***

490 SNP variants were identified between *T. rubrum* isolates to examine the level of
491 divergence within this species complex (**Table S8**). On average, *T. rubrum* isolates
492 contain 8,092 SNPs compared to the reference genome of the CBS118892 isolate; this
493 reflects a bimodal divergence pattern where most isolates including three morphotypes
494 (*fischeri*, *kanei*, and *raubitscheckii*) have an average of 3,930 SNPs and two more
495 divergent isolates (morphotypes *megninii* and *soudanense*) have an average of 24,740
496 SNPs. The average nucleotide diversity (π) for all 10 *T. rubrum* isolates is 0.00054;
497 excluding the two divergent morphotypes, the average nucleotide diversity is 0.00031.
498 By comparison, the average nucleotide diversity of the fungal pathogen *Cryptococcus*
499 *neoformans* var. *grubii*, which is actively recombining as evidenced by low linkage
500 disequilibrium (Desjardins *et al.* 2017; Rhodes *et al.* 2017), is 0.0074, a level
501 approximately 24-fold higher than that in *T. rubrum* (**Methods**, (Rhodes *et al.* 2017)).
502 Even higher levels of nucleotide diversity have been reported in global populations of
503 other fungi (see **Discussion**). A similar magnitude of SNPs separate the two *T.*
504 *interdigitale* isolates; 22,568 SNPs were identified based on the alignment of H6 reads
505 to the MR 816 assembly. Across all isolates, SNPs were predominantly found in
506 intergenic regions for both species, representing 76% and 81% of total variants
507 respectively (**Table 1**, **Table S8**). Within genes, the higher ratio of nonsynonymous
508 relative to synonymous changes among the closely related *T. rubrum* isolates (**Table 1**)

509 is consistent with lower purifying selection over recent evolutionary time (Rocha *et al.*
510 2006).

511
512 Examining the frequency of SNPs across the *T. rubrum* genome revealed high diversity
513 regions that flank the mating type locus in the two divergent isolates. Across all isolates,
514 some regions of the genome are over-represented for SNPs, including the smallest
515 scaffolds of the reference genome (**Figure 5**); these regions contain a high fraction of
516 repetitive elements (Martinez *et al.* 2012). The largest high diversity window unique to
517 the *T. rubrum* morphotype *megrinii* was found in an ~810-kb region encompassing the
518 mating type locus on scaffold 2; a smaller high diversity region spanning the mating type
519 locus was found in the diverged *soudandense* isolate (**Figure 5**). The higher diversity
520 found in this location could reflect introgressed regions from recent outcrossing or could
521 be associated with lower recombination proximal to the mating type locus, resulting in
522 stratification of linked genes.

523

524 **Gene content variation in *T. rubrum* and *T. interdigitale***

525 To examine variation in gene content in the *Trichophyton rubrum* species complex, we
526 first measured copy number variation across the genome. Duplicated and deleted
527 regions of the genome were identified based on significant variation in normalized read
528 depth (Methods). We observed increased copy number only for two adjacent 26 kb
529 regions of scaffold 4 in two isolates (MR850 and MR1448) (**Figure S6**). Both of these
530 regions had nearly triploid levels of coverage (**Table S9**). While ploidy variation is a
531 mechanism of drug resistance in fungal pathogens, none of the 25 total genes in these
532 regions (**Table S10**) are known drug targets or efflux pumps. These regions include two
533 genes classified as fungal zinc cluster transcription factors; this family of transcription
534 factors was previously noted to vary in number between dermatophyte species
535 (Martinez *et al.* 2012). A total of 12 deleted regions (CNVnator p-val <0.01) ranging in
536 size from 4 to 37 kb were also identified in a subset of genomes (**Table S11**). Two of
537 these regions include genes previously noted to have higher copy number in
538 dermatophyte genomes, a nonribosomal peptide synthase (NRPS) gene
539 (TERG_02711) and a LysM gene (TERG_02813) (**Table S12**). Overall this analysis

540 suggests recent gain or loss in dermatophytes for a small set of genes including
541 transcription factors, NRPS, and LysM domain proteins.

542 We next examined candidate loss of function mutations in the *T. rubrum* species
543 complex. For the 8 closely related *T. rubrum* isolates, an average of 8.1 SNPs are
544 predicted to result in new stop codons, disrupting protein coding regions; in the
545 *soudanense* and *megrinii* isolates, an average of 58.5 SNPs result in new stop codons.
546 These predicted loss of function mutations do not account for previously noted
547 phenotypic differences between the morphotypes; no stop codons were found in the
548 seven genes involved in histidine biosynthesis (*HIS1-HIS7*) in the histidine auxotroph *T.*
549 *rubrum* morphotype *megrinii* or in urease genes in *T. rubrum* morphotype
550 *raubitscheckii*.

551

552 Comparison of the first representative genomes for *T. interdigitale* (isolates MR816 and
553 H6) to those of dermatophyte species highlighted the close relationship of *T.*
554 *interdigitale* to *T. tonsurans* and *T. equinum*. These three species are closely related
555 (**Figure 2**), sharing 7,618 ortholog groups, yet there are also substantial differences in
556 gene content. A total of 1,253 orthologs groups were present only in *T. equinum* and *T.*
557 *tonsurans* and 512 ortholog groups were present only in both *T. interdigitale* isolates.
558 However, there were no significant differences in functional groups between these
559 species based on PFAM domain analysis, suggesting no substantial gain or loss of
560 specific protein families. Two PFAM domains were unique to the *T. interdigitale* isolates
561 and present in more than one copy: PF00208, found in ELFV dehydrogenase family
562 members and PF00187, a chitin recognition protein domain. This chitin binding domain
563 is completely absent from the *T. equinum* and *T. tonsurans* genomes while in *T.*
564 *interdigitale* this domain is associated with the glycosyl hydrolase family 18 (GH18)
565 domain (Davies and Henrissat 1995). GH18 proteins are chitinases and some other
566 members of this family also contain LysM domains. We also examined genes in the
567 ergosterol pathway for variation, as this could relate to drug resistance; while this
568 pathway is highly conserved in dermatophytes (Martinez *et al.* 2012), *T. interdigitale*
569 isolates had an extra copy of a gene containing the ERG4/ERG24 domain found in
570 sterol reductase enzymes in the ergosterol biosynthesis pathway. The *ERG4* gene

571 encodes an enzyme that catalyzes the final step in ergosterol biosynthesis, and it is
572 possible that an additional copy of this gene results in higher protein levels to help
573 ensure that this step is not rate limiting.

574
575 These comparisons also highlighted the recent dynamics of the LysM family, which
576 binds bacterial peptidoglycan and fungal chitin (Buist *et al.* 2008). Dermatophytes
577 contain high numbers of LysM domain proteins ranging from the 10 genes found in *T.*
578 *verrucosum* to 31 copies found in *M. canis* (**Table S13**, (Martinez *et al.* 2012)). Both the
579 class of LysM proteins with additional catalytic domains and the larger class consists of
580 proteins with only LysM domains, many of which contain secretion signals and may
581 represent candidate effectors (Martinez *et al.* 2012), vary in number across the
582 dermatophytes. Isolates from the *T. rubrum* species complex have 16 to 18 copies of
583 LysM proteins compared to the 15 found in the previously reported genome of the CBS
584 118892 isolate (**Table S13**). One of the additional LysM genes present in all of the
585 newly sequenced isolates encodes a polysaccharide deacetylase domain involved in
586 chitin catabolism. There is also an additional copy of a gene with only a LysM domain in
587 9 of the 10 new *T. rubrum* isolates (**Table S13**). The genomes of the *T. interdigitale*
588 isolates have only 14 genes containing a LysM binding domain, and are missing a LysM
589 gene encoding GH18 and Hce2 domains (**Figure S7**). Notably, this locus is closely
590 linked to genes encoding additional LysM domain proteins in some species (**Figure S7**).
591 The variation observed in the LysM gene family suggests that recognition of chitin
592 appears to be highly dynamic based on these differences in gene content and domain
593 composition.

594

595 **Discussion**

596

597 In this study, we selected diverse *T. rubrum* isolates for genome sequencing, assembly,
598 and analysis and surveyed a wider population sample using MLST analysis. These
599 isolates include multiple morphotypes, which show noted phenotypic variation yet are
600 assigned to the same species based on phylogenetic analyses (Gräser *et al.* 2008; de
601 Hoog *et al.* 2017a). The *T. rubrum* morphotype *soudanense* and *T. rubrum* morphotype

602 *megninii* show higher divergence from a closely related subgroup that includes the
603 *kanei*, *raubitschekii*, and *fischerii* morphotypes, as well as most other *T. rubrum* isolates.

604
605 Our MLST and whole genome analyses provide strong support that *T. rubrum* is highly
606 clonal and may be primarily asexual or at least infrequently sexually reproducing.
607 Across 135 isolates examined, 134 were from a single mating type (*MAT1-1*). Only the
608 *T. rubrum* type *megninii* isolate, Consistent with prior reports (Gräser *et al.* 2008; de
609 Hoog *et al.* 2017a p. 201), only the *T. rubrum* morphotype *megninii* isolates contains the
610 opposite mating type (*MAT1-2*) while all other *T. rubrum* isolates that are of *MAT1-1*
611 type. Direct tests of mating between these and other species did not find evidence for
612 mating and sexual development. While mating was not detected, studies in other fungi
613 have required specialized conditions and long periods of time to detect sexual
614 reproduction (O’Gorman *et al.* 2009). As genes involved in mating and meiosis are
615 conserved in *T. rubrum* (Martinez *et al.* 2012), gene loss does not provide a simple
616 explanation for the inability to mate. Sexual reproduction might occur rarely under
617 specific conditions such as specific temperatures as found for *Trichophyton onychocola*
618 (Hubka *et al.* 2015), may be geographically restricted, as the opposite mating type
619 *megninii* morphotype is generally found in the Mediterranean (Sequeira *et al.* 1991), or
620 could be unisexual as in some other fungi such as *Cryptococcus neoformans* (Lin *et al.*
621 2005).

622
623 As MLST data provided no resolution of the substructure of the *T. rubrum* population,
624 we examined whole genome sequences for 8 diverse isolates. Analysis of the sequence
625 read depth revealed that while some small regions of the genome show amplification or
626 loss, there is no evidence for aneuploidy of entire chromosomes. Most of these *T.*
627 *rubrum* isolates contain an average of only 3,930 SNPs (0.01% of the genome) and
628 phylogenetic analysis revealed little genetic substructure. Two isolates were more
629 divergent with an average of 24,740 SNPs (0.06% of the genome); one of these was of
630 the recently proposed separated species *T. soudanense* (de Hoog *et al.* 2017a), and
631 the other was the *T. rubrum* morphotype *megninii* isolate. While the similar level of
632 divergence raises the question of whether morphotype *megninii* isolates could also be a

633 separate species, this has not yet been proposed when considering additional
634 phenotypic data in addition to molecular data, however further study would help clarify
635 species assignments. The low level of variation is remarkable in comparison to other
636 fungal pathogens; for example, while *T. rubrum* isolates are identical at 99.97% of
637 positions on average, isolates of *Cryptococcus neoformans* var. *grubii* isolates are
638 99.36% identical on average (Desjardins *et al.* 2017; Rhodes *et al.* 2017). Global
639 populations of *Saccharomyces* have even higher reported diversity (Liti *et al.* 2009). The
640 low diversity and the dependency on the human host for growth suggests that *T. rubrum*
641 may have a low effective population size impacted by the reduction of intra-species
642 variation by genetic drift. In addition, direct tests for recombination found a low level of
643 candidate reassortments that was not in excess of the estimated number of
644 homoplasmic mutations; further, as there was no apparent decay of linkage
645 disequilibrium over genetic distance, our analyses support the overall clonal nature of
646 this species. The high clonality observed in *T. rubrum* is also supported by MLST
647 analysis of eight microsatellite markers in approximately 230 *T. rubrum* isolates,
648 including morphotypes from diverse geographic origins (Gräser *et al.* 2007). With
649 additional genome sequencing geographic substructure may become more apparent;
650 the fungal pathogen *Talaromyces marneffeii* also displays high clonality yet isolates from
651 the same country or region are more closely related (Henk *et al.* 2012). While low
652 levels of diversity seems surprising in a common pathogen, this is similar to findings in
653 some bacterial pathogens including *Mycobacterium tuberculosis* and *Mycobacterium*
654 *leprae* (Monot *et al.* 2005; Comas *et al.* 2013), which also display high clonality despite
655 phenotypic variation.

656
657 LysM domain proteins are involved in dampening host recognition of fungal chitin (de
658 Jonge *et al.* 2010) and can also regulate fungal growth and development (Seidl-Seiboth
659 *et al.* 2013), yet their specific function in dermatophytes and closely related fungi is not
660 well understood. We also observed variation in genes containing the LysM domain
661 across the sequenced isolates, both in the gene number and domain organization.
662 LysM genes are present in higher copy number in dermatophytes than related fungi in
663 the Ascomycete order Onygenales (Martinez *et al.* 2012). Recent sequencing of

664 additional non-pathogenic species in this order related to *Coccidioides* revealed that
665 most LysM copies found in dermatophytes have a homolog (Whiston and Taylor 2015).
666 Although this analysis excluded *M. canis* — the dermatophyte species with the highest
667 LysM count— this suggests that dermatophytes have retained rather than recently
668 duplicated many of their LysM genes. However, changes in the domain composition of
669 both genes with catalytic domains and those with only LysM domains, many of which
670 represent candidate effectors, highlights the dynamic evolution of the LysM family in the
671 dermatophytes. Studies of LysM genes in dermatophytes are needed to determine
672 whether these genes serve similar or different roles in these species.

673

674 *T. rubrum* is only found as a pathogen of humans, though this adaptation is more recent
675 relative to the related species that infect other animals or grow in the environment.
676 Unlike the obligate human fungal pathogen *Pneumocystis jirovecii* (Cissé *et al.* 2012;
677 Ma *et al.* 2016), *T. rubrum* does not display widespread gene loss (Martinez *et al.* 2012)
678 indicative of host dependency for growth; further, its genome size is also comparable to
679 related dermatophyte species, supporting no overall reduction (Martinez *et al.* 2012).
680 The presence of a single mating type in the vast majority of isolates and limited
681 evidence of recombination suggests that sexual reproduction of *T. rubrum* may have
682 been recently lost or may be rarely occurring in specific conditions or geographic
683 regions. This may be linked to the specialization as a human pathogen, as mating may
684 be optimized during environmental growth in the soil (Gräser *et al.* 2008).

685

686

687 **Acknowledgements**

688 We thank the Broad Institute Genomics Platform for generating the DNA sequence
689 described here. We thank Yonathan Lewit for technical assistance and Cecelia Wall for
690 providing helpful comments on the manuscript. Financial support was provided by the
691 National Human Genome Research Institute grant number U54HG003067 to the Broad
692 Institute and by NIH/NIAID R37 MERIT Award AI39115-20 and RO1 Award AI50113-13
693 to JH. This study was supported by The Scientific and Technological Research Council
694 of Turkey-2219 Research Fellowship Programme for International Researchers Project

695 No. [1059B191501539] to AD and Brazilian funding agency FAPESP Fundação de
696 Amparo à Pesquisa do Estado de São Paulo, Postdoctoral Fellowship 12/22232-8 and
697 13/19195-6 to GFP.

698

699 **Author contributions**

700 C.A.C., D.A.M., T.C.W. and J.H. conceived and designed the project. A.D., B.M, S.H.,

701 M. I., R.B., B.O., Y.G, N.M.M, and T.W. provided the isolates. W.L. and A.D. performed

702 the laboratory experiments. G.F.P, D.A.M, W.L, A.D., R.B.B, A.A, J.M., G,T.S., S.Y,

703 Q.Z, and C.A.C analyzed the data. C.A.C. and J.H. wrote the paper with input from all

704 authors. C.A.C. and J.H. supervised and coordinated the project.

705

706

707

708 **References**

- 709 Abyzov A., Urban A. E., Snyder M., Gerstein M., 2011 CNVnator: an approach to
710 discover, genotype, and characterize typical and atypical CNVs from family and
711 population genome sequencing. *Genome Res.* 21: 974–984.
- 712 Achterman R. R., White T. C., 2013 Dermatophytes. *Curr. Biol.* 23: R551-552.
- 713 Altschul S. F., Madden T. L., Schaffer A. A., Zhang J., Zhang Z., *et al.*, 1997 Gapped
714 BLAST and PSI-BLAST: a new generation of protein database search programs.
715 *Nucleic Acids Res* 25: 3389–402.
- 716 Anzawa K., Kawasaki M., Mochizuki T., Ishizaki H., 2010 Successful mating of
717 *Trichophyton rubrum* with *Arthroderma simii*. *Med. Mycol. Off. Publ. Int. Soc.*
718 *Hum. Anim. Mycol.* 48: 629–34.
- 719 Birney E., Clamp M., Durbin R., 2004 GeneWise and Genomewise. *Genome Res* 14:
720 988–95.
- 721 Borodovsky M., Lomsadze A., Ivanov N., Mills R., 2003 Eukaryotic gene prediction
722 using GeneMark.hmm. *Curr Protoc Bioinforma.* Chapter 4: Unit4 6.
- 723 Buist G., Steen A., Kok J., Kuipers O. P., 2008 LysM, a widely distributed protein motif
724 for binding to (peptido)glycans. *Mol. Microbiol.* 68: 838–847.
- 725 Burmester A., Shelest E., Glockner G., Heddergott C., Schindler S., *et al.*, 2011
726 Comparative and functional genomics provide insights into the pathogenicity of
727 dermatophytic fungi. *Genome Biol.* 12: R7.
- 728 Cervelatti E. P., Fachin A. L., Ferreira-Nozawa M. S., Martinez-Rossi N. M., 2006
729 Molecular cloning and characterization of a novel ABC transporter gene in the
730 human pathogen *Trichophyton rubrum*. *Med. Mycol.* 44: 141–147.
- 731 Cissé O. H., Pagni M., Hauser P. M., 2012 De novo assembly of the *Pneumocystis*
732 *jirovecii* genome from a single bronchoalveolar lavage fluid specimen from a
733 patient. *mBio* 4: e00428-00412.
- 734 Comas I., Coscolla M., Luo T., Borrell S., Holt K. E., *et al.*, 2013 Out-of-Africa migration
735 and Neolithic coexpansion of *Mycobacterium tuberculosis* with modern humans.
736 *Nat. Genet.* 45: 1176–1182.
- 737 Danecek P., Auton A., Abecasis G., Albers C. A., Banks E., *et al.*, 2011 The variant call
738 format and VCFtools. *Bioinforma. Oxf. Engl.* 27: 2156–2158.
- 739 Davies G., Henrissat B., 1995 Structures and mechanisms of glycosyl hydrolases.
740 *Struct. Lond. Engl.* 1993 3: 853–859.
- 741 Desjardins C. A., Giamberardino C., Sykes S. M., Yu C.-H., Tenor J. L., *et al.*, 2017
742 Population genomics and the evolution of virulence in the fungal pathogen
743 *Cryptococcus neoformans*. *Genome Res.* 27: 1207–1219.
- 744 Eddy S. R., 2011 Accelerated Profile HMM Searches. *PLoS Comput. Biol.* 7: e1002195.
- 745 Edgar R. C., 2004 MUSCLE: multiple sequence alignment with high accuracy and high
746 throughput. *Nucleic Acids Res* 32: 1792–7.

- 747 Finn R. D., Bateman A., Clements J., Coggill P., Eberhardt R. Y., *et al.*, 2014 Pfam: the
748 protein families database. *Nucleic Acids Res.* 42: D222-230.
- 749 Fisher S., Barry A., Abreu J., Minie B., Nolan J., *et al.*, 2011 A scalable, fully automated
750 process for construction of sequence-ready human exome targeted capture
751 libraries. *Genome Biol.* 12: R1.
- 752 Gnerre S., Maccallum I., Przybylski D., Ribeiro F. J., Burton J. N., *et al.*, 2011 High-
753 quality draft assemblies of mammalian genomes from massively parallel
754 sequence data. *Proc Natl Acad Sci U A* 108: 1513–8.
- 755 Grabherr M. G., Haas B. J., Yassour M., Levin J. Z., Thompson D. A., *et al.*, 2011 Full-
756 length transcriptome assembly from RNA-Seq data without a reference genome.
757 *Nat. Biotechnol.* 29: 644–652.
- 758 Gräser Y., Kuijpers A. F., Presber W., Hoog G. S. de, 2000 Molecular taxonomy of the
759 *Trichophyton rubrum* complex. *J. Clin. Microbiol.* 38: 3329–3336.
- 760 Gräser Y., Fröhlich J., Presber W., Hoog S. de, 2007 Microsatellite markers reveal
761 geographic population differentiation in *Trichophyton rubrum*. *J. Med. Microbiol.*
762 56: 1058–1065.
- 763 Gräser Y., Scott J., Summerbell R., 2008 The new species concept in dermatophytes-a
764 polyphasic approach. *Mycopathologia* 166: 239–56.
- 765 Haas B. J., Delcher A. L., Mount S. M., Wortman J. R., Smith R. K., *et al.*, 2003
766 Improving the Arabidopsis genome annotation using maximal transcript
767 alignment assemblies. *Nucleic Acids Res* 31: 5654–66.
- 768 Haas B. J., Salzberg S. L., Zhu W., Pertea M., Allen J. E., *et al.*, 2008 Automated
769 eukaryotic gene structure annotation using EVIDENCEModeler and the Program to
770 Assemble Spliced Alignments. *Genome Biol.* 9: R7.
- 771 Haas B. J., Zeng Q., Pearson M. D., Cuomo C. A., Wortman J. R., 2011 Approaches to
772 fungal genome annotation. *Mycology* 2: 118–141.
- 773 Hall T., 1999 BioEdit: a user-friendly biological sequence alignment editor and analysis
774 program for Windows 95/98/NT. *Nucleic Acids Symp. Ser.* 41: 95–98.
- 775 Heidemann S., Monod M., Gräser Y., 2010 Signature polymorphisms in the internal
776 transcribed spacer region relevant for the differentiation of zoophilic and
777 anthropophilic strains of *Trichophyton interdigitale* and other species of
778 *T. mentagrophytes sensu lato*. *Br. J. Dermatol.* 162: 282–295.
- 779 Heitman J., 2010 Evolution of eukaryotic microbial pathogens via covert sexual
780 reproduction. *Cell Host Microbe* 8: 86–99.
- 781 Henk D. A., Shahar-Golan R., Devi K. R., Boyce K. J., Zhan N., *et al.*, 2012 Clonality
782 despite sex: the evolution of host-associated sexual neighborhoods in the
783 pathogenic fungus *Penicillium marneffeii*. *PLoS Pathog.* 8: e1002851.
- 784 Hoog G. S. de, Dukik K., Monod M., Packeu A., Stubbe D., *et al.*, 2017a Toward a novel
785 multilocus phylogenetic taxonomy for the dermatophytes. *Mycopathologia* 182:
786 5–31.

787 Hoog S. de, Monod M., Dawson T., Boekhout T., Mayser P., *et al.*, 2017b Skin Fungi
788 from Colonization to Infection. *Microbiol. Spectr.* 5.

789 Hubka V., Nissen C. V., Jensen R. H., Arendrup M. C., Cmokova A., *et al.*, 2015
790 Discovery of a sexual stage in *Trichophyton onychocola*, a presumed geophilic
791 dermatophyte isolated from toenails of patients with a history of *T. rubrum*
792 onychomycosis. *Med. Mycol.* 53: 798–809.

793 Jonge R. de, Esse H. P. van, Kombrink A., Shinya T., Desaki Y., *et al.*, 2010 Conserved
794 fungal LysM effector Ecp6 prevents chitin-triggered immunity in plants. *Science*
795 329: 953–5.

796 Jurka J., Kapitonov V. V., Pavlicek A., Klonowski P., Kohany O., *et al.*, 2005 Repbase
797 Update, a database of eukaryotic repetitive elements. *Cytogenet Genome Res*
798 110: 462–7.

799 Kane J., Salkin I. F., Weitzman I., Smitka C., *Trichophyton raubitschekii*, sp. nov.
800 *Mycotaxon* 13: 259–266.

801 Kano R., Isizuka M., Hiruma M., Mochizuki T., Kamata H., *et al.*, 2013 Mating type gene
802 (*MAT1-1*) in Japanese isolates of *Trichophyton rubrum*. *Mycopathologia* 175:
803 171–173.

804 Kent W. J., 2002 BLAT--the BLAST-like alignment tool. *Genome Res* 12: 656–64.

805 Korf I., 2004 Gene finding in novel genomes. *BMC Bioinformatics* 5: 59.

806 Kurtz S., Phillippy A., Delcher A. L., Smoot M., Shumway M., *et al.*, 2004 Versatile and
807 open software for comparing large genomes. *Genome Biol* 5: R12.

808 Lagesen K., Hallin P., Rodland E. A., Staerfeldt H. H., Rognes T., *et al.*, 2007
809 RNAmmer: consistent and rapid annotation of ribosomal RNA genes. *Nucleic*
810 *Acids Res* 35: 3100–8.

811 Li L., Stoeckert C. J., Roos D. S., 2003 OrthoMCL: identification of ortholog groups for
812 eukaryotic genomes. *Genome Res* 13: 2178–89.

813 Li W., Metin B., White T. C., Heitman J., 2010 Organization and evolutionary trajectory
814 of the mating type (*MAT*) locus in dermatophyte and dimorphic fungal pathogens.
815 *Eukaryot Cell* 9: 46–58.

816 Li H., 2013 Aligning sequence reads, clone sequences and assembly contigs with BWA-
817 MEM. *ArXiv13033997 Q-Bio*.

818 Lin X., Hull C. M., Heitman J., 2005 Sexual reproduction between partners of the same
819 mating type in *Cryptococcus neoformans*. *Nature* 434: 1017–1021.

820 Liti G., Carter D. M., Moses A. M., Warringer J., Parts L., *et al.*, 2009 Population
821 genomics of domestic and wild yeasts. *Nature* 458: 337–41.

822 Lowe T. M., Eddy S. R., 1997 tRNAscan-SE: a program for improved detection of
823 transfer RNA genes in genomic sequence. *Nucleic Acids Res* 25: 955–64.

824 Ma L., Chen Z., Huang D. W., Kutty G., Ishihara M., *et al.*, 2016 Genome analysis of
825 three *Pneumocystis* species reveals adaptation mechanisms to life exclusively in
826 mammalian hosts. *Nat. Commun.* 7: 10740.

- 827 Majoros W. H., Pertea M., Salzberg S. L., 2004 TigrScan and GlimmerHMM: two open
828 source ab initio eukaryotic gene-finders. *Bioinforma. Oxf. Engl.* 20: 2878–2879.
- 829 Martinez D. A., Oliver B. G., Gräser Y., Goldberg J. M., Li W., *et al.*, 2012 Comparative
830 genome analysis of *Trichophyton rubrum* and related dermatophytes reveals
831 candidate genes involved in infection. *mBio* 3: e00259-00212.
- 832 McKenna A., Hanna M., Banks E., Sivachenko A., Cibulskis K., *et al.*, 2010 The
833 Genome Analysis Toolkit: a MapReduce framework for analyzing next-generation
834 DNA sequencing data. *Genome Res* 20: 1297–303.
- 835 Metin B., Heitman J., 2017 Sexual reproduction in dermatophytes. *Mycopathologia* 182:
836 45–55.
- 837 Monot M., Honoré N., Garnier T., Araoz R., Coppée J.-Y., *et al.*, 2005 On the origin of
838 leprosy. *Science* 308: 1040–1042.
- 839 O’Gorman C. M., Fuller H. T., Dyer P. S., 2009 Discovery of a sexual cycle in the
840 opportunistic fungal pathogen *Aspergillus fumigatus*. *Nature* 457: 471–4.
- 841 Ren X., Liu T., Dong J., Sun L., Yang J., *et al.*, 2012 Evaluating de Bruijn graph
842 assemblers on 454 transcriptomic data. *PLoS ONE* 7: e51188.
- 843 Rhodes J., Desjardins C. A., Sykes S. M., Beale M. A., Vanhove M., *et al.*, 2017 Tracing
844 Genetic Exchange and Biogeography of *Cryptococcus neoformans* var. *grubii* at
845 the Global Population Level. *Genetics* 207: 327–346.
- 846 Rocha E. P. C., Smith J. M., Hurst L. D., Holden M. T. G., Cooper J. E., *et al.*, 2006
847 Comparisons of dN/dS are time dependent for closely related bacterial genomes.
848 *J. Theor. Biol.* 239: 226–235.
- 849 Seidl-Seiboth V., Zach S., Frischmann A., Spadiut O., Dietzsch C., *et al.*, 2013 Spore
850 germination of *Trichoderma atroviride* is inhibited by its LysM protein TAL6.
851 *FEBS J.* 280: 1226–1236.
- 852 Sequeira H., Cabrita J., De Vroey C., Wuytack-Raes C., 1991 Contribution to our
853 knowledge of *Trichophyton megninii*. *J. Med. Vet. Mycol. Bi-Mon. Publ. Int. Soc.*
854 *Hum. Anim. Mycol.* 29: 417–418.
- 855 Stamatakis A., 2006 RAxML-VI-HPC: maximum likelihood-based phylogenetic analyses
856 with thousands of taxa and mixed models. *Bioinformatics* 22: 2688–90.
- 857 Stanke M., Steinkamp R., Waack S., Morgenstern B., 2004 AUGUSTUS: a web server
858 for gene finding in eukaryotes. *Nucleic Acids Res* 32: W309-12.
- 859 Storey J. D., Tibshirani R., 2003 Statistical significance for genomewide studies. *Proc*
860 *Natl Acad Sci U A* 100: 9440–5.
- 861 Symoens F., Jousson O., Packeu A., Fratti M., Staib P., *et al.*, 2013 The dermatophyte
862 species *Arthroderma benhamiae*: intraspecies variability and mating behaviour.
863 *J. Med. Microbiol.* 62: 377–385.
- 864 Turin L., Riva F., Galbiati G., Cainelli T., 2000 Fast, simple and highly sensitive double-
865 rounded polymerase chain reaction assay to detect medically relevant fungi in
866 dermatological specimens. *Eur. J. Clin. Invest.* 30: 511–518.

- 867 Weitzman I., Silva-Hutner M., 1967 Non-keratinous agar media as substrates for the
868 ascigerous state in certain members of the Gymnoascaceae pathogenic for man
869 and animals. *Sabouraudia* 5: 335–340.
- 870 Whiston E., Taylor J. W., 2015 Comparative phylogenomics of pathogenic and
871 nonpathogenic species. *G3 Bethesda Md* 6: 235–244.
- 872 White T. C., Oliver B. G., Gräser Y., Henn M. R., 2008 Generating and testing molecular
873 hypotheses in the dermatophytes. *Eukaryot. Cell* 7: 1238–45.
- 874 White T. C., Findley K., Dawson T. L., Scheynius A., Boekhout T., *et al.*, 2014 Fungi on
875 the Skin: Dermatophytes and *Malassezia*. *Cold Spring Harb. Perspect. Med.* 4.
- 876 Wu C. H., Apweiler R., Bairoch A., Natale D. A., Barker W. C., *et al.*, 2006 The
877 Universal Protein Resource (UniProt): an expanding universe of protein
878 information. *Nucleic Acids Res.* 34: D187–D191.
- 879 Yang Z., 2007 PAML 4: phylogenetic analysis by maximum likelihood. *Mol. Biol. Evol.*
880 24: 1586–1591.
- 881 Young C. N., 1968 Pseudo-Cleistothecia in *Trichophyton rubrum*. *Sabouraudia J. Med.*
882 *Vet. Mycol.* 6: 160–162.
- 883
- 884

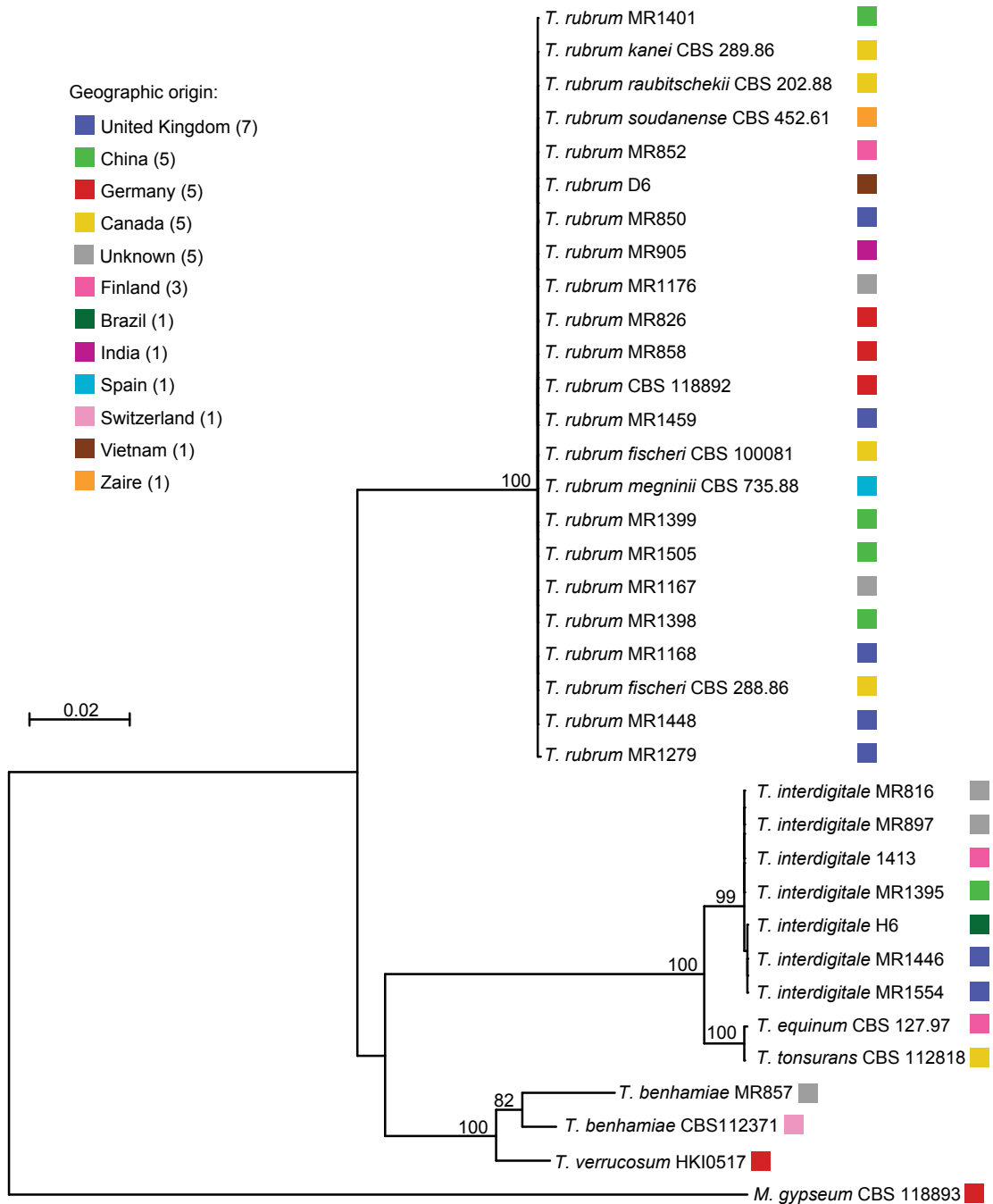
885 **Table****Table 1. Variation in *T. rubrum* SNP rate and class**

Isolate	Total Number of SNPs	SNPs in CDS*	SYN*	NSY*	pN/pS*
<i>T. rubrum</i> MR1448	4,283	374	83	287	1.15
<i>T. rubrum</i> MR1459	2,188	436	103	317	1.02
<i>T. rubrum</i> MR850	4,203	387	88	289	1.09
<i>T. rubrum</i> D6	4,121	484	112	363	1.08
<i>T. rubrum</i> (morphotype <i>fischeri</i>) CBS 100081	4,199	409	94	307	1.09
<i>T. rubrum</i> (morphotype <i>fischeri</i>) CBS 288.86	4,147	375	84	283	1.12
<i>T. rubrum</i> (morphotype <i>kanei</i>) CBS 289.86	4,491	474	116	350	1.00
<i>T. rubrum</i> (morphotype <i>raubitschekii</i>) CBS 202.88	3,808	375	83	285	1.14
<i>T. rubrum</i> (morphotype <i>megninii</i>) CBS 735.88	26,406	7,328	3,069	4,185	0.45
<i>T. rubrum</i> (morphotype <i>soudanense</i>) CBS 452.61	23,073	6,253	2,377	3,808	0.53
<i>T. interdigitale</i> MR816	1,223,298	591,173	395,250	194,498	0.16
<i>T. interdigitale</i> H6	1,183,411	585,288	393,079	190,826	0.16

886 *CDS, coding sequence; SYN, synonymous SNP sites; NSY, non-synonymous SNP sites; pN/pS, (NSY/total NSY
887 sites)/(SYN/total SYN sites).

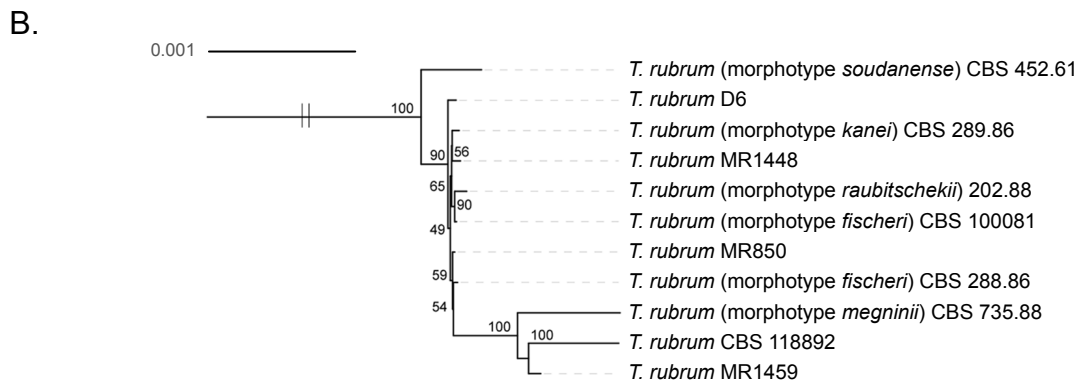
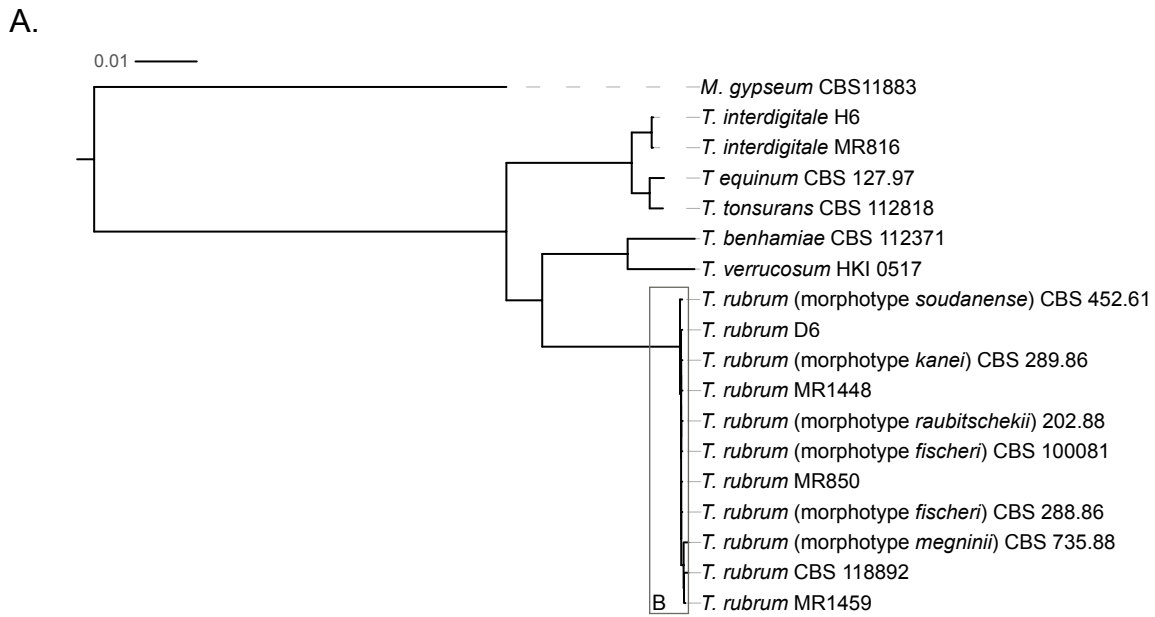
888

889



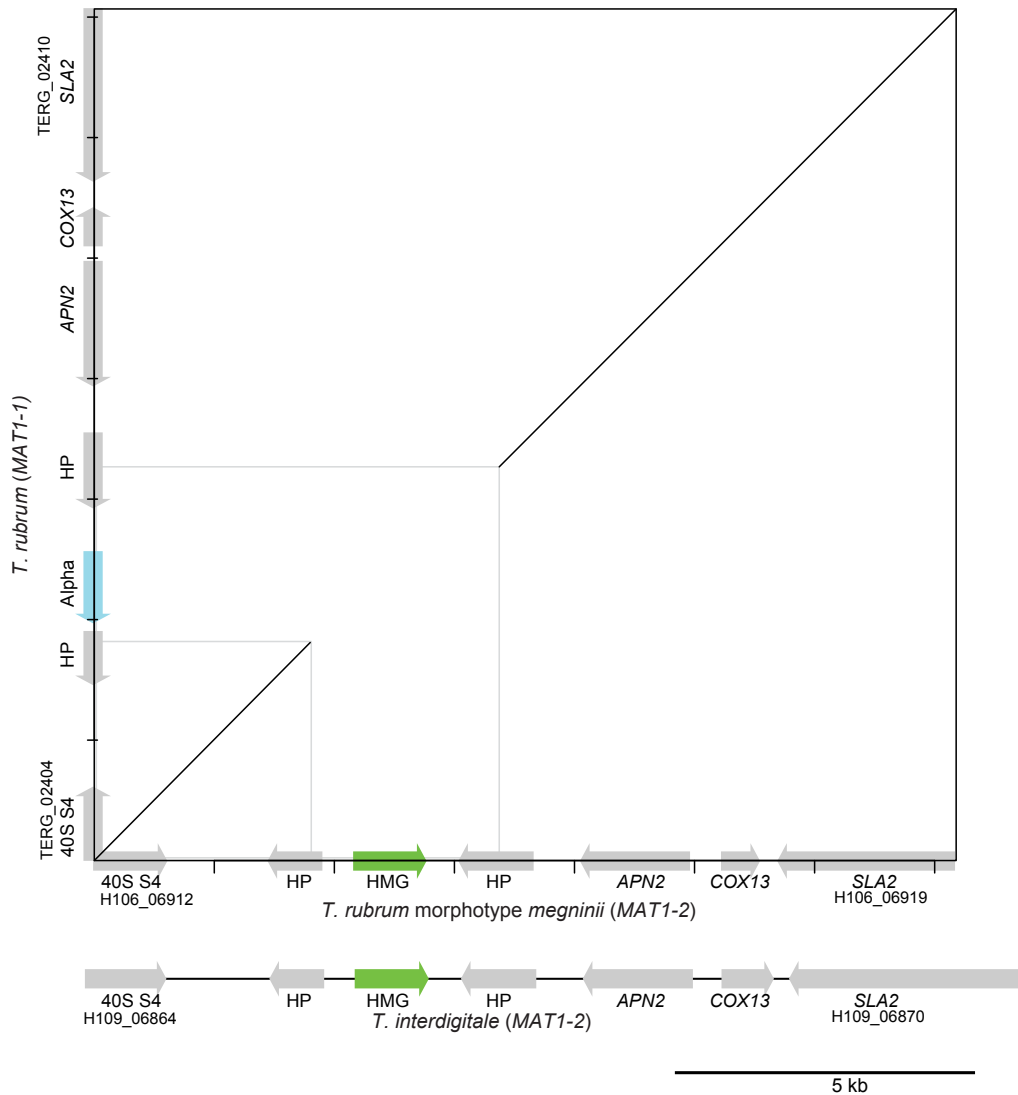
890

891 **Figure 1.** Phylogeny inferred from concatenated MLST sequences. Three MLST loci
 892 (ABC transporter, outer membrane protein, and CAP59 protein) were amplified and
 893 sequenced from 79 isolates and sequences were identified in an additional 19
 894 assemblies. The concatenated sequence for each isolate was used to build a maximum
 895 likelihood tree using MEGA 5.2. Isolate MR1168 is representative of 73 *T. rubrum*
 896 isolates that have identical MLST sequences.

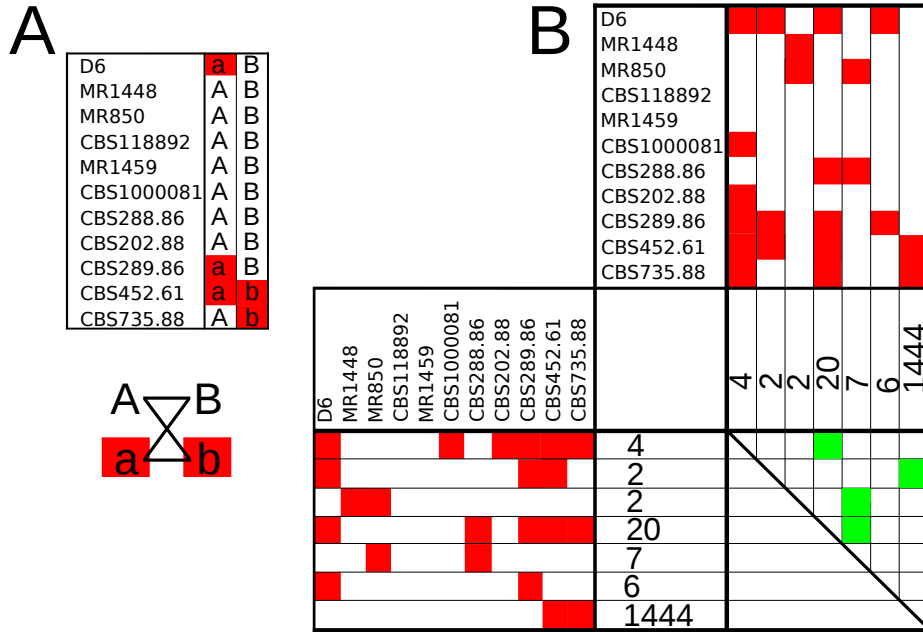


897
 898 **Figure 2.** Phylogenetic relationship of *Trichophyton* isolates. A total of 5,236 single copy
 899 genes were each aligned with MUSCLE; the concatenated alignment was used to infer
 900 a species phylogeny with RAxML (GTRCAT model) with 1,000 bootstrap replicates
 901 using either A. all species including the outgroup *M. gypseum* or B. only *Trichophyton*
 902 *rubrum* isolates.

903
 904

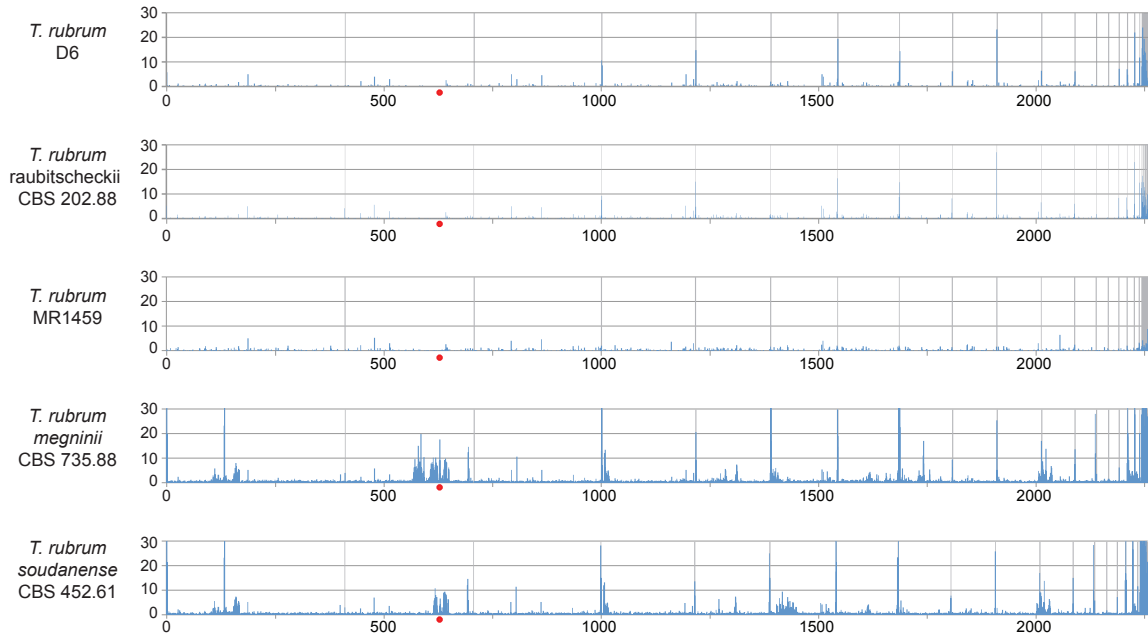


905
 906 **Figure 3.** Alignment of the mating type locus of selected isolates. Mating type genes of
 907 *T. rubrum* morphotype *megninii* (CBS 735.88) and *T. rubrum* (CBS 188992) are shown
 908 along the x- and y- axes, respectively, with regions aligning by NUCmer show in the
 909 dotplot. The alignment extends into two hypothetical proteins (HP) immediately flanking
 910 the alpha or HMG domain gene that specifies mating type. Most *T. rubrum* (*MAT1-1*)
 911 isolates contain an alpha domain protein (blue) at the *MAT* locus. In contrast, the *T.*
 912 *rubrum* morphotype *megninii* isolate contains an HMG domain protein (green)
 913 representing the opposite mating type (*MAT1-2*). All sequenced *T. interdigitale*
 914 isolates are also of *MAT1-2* mating type including MR816. Gene locus identifiers are shown for
 915 the genes flanking each locus (prefix TERG, H106, and H109).
 916
 917



918
 919 **Figure 4.** Paired allele compatibility test suggests limited evidence for sexual
 920 reproduction. A. A single example of a positive paired allele compatibility test from the
 921 *T. rubrum* population. In this test, two loci are examined and typed across the
 922 population. To perform a meaningful test, at least two individuals in the population must
 923 share a variant allele at each site. Here alternative SNPs are depicted in red and
 924 reference in white. Evidence for recombination is provided by any pairwise comparison
 925 of two loci in which isolates are present where red-red, white-white, red-white, and
 926 white-red combinations are all found (AB, Ab, aB, and ab) satisfying the allele
 927 compatibility test and providing evidence for recombination. B. Paired allele
 928 compatibility tests were performed for all isolates in the *T. rubrum* population across the
 929 entire genome. SNP profiles were grouped into unique and informative allele patterns
 930 and collapsed, with the number of occurrences of each profile across the genome listed.
 931 Thus, the larger the number, the more common that SNP distribution is in the
 932 population. Pairwise tests were then conducted for each combination of SNP profiles.
 933 Reference nucleotides are indicated by white and variant by red. The pairwise matrix
 934 displays the results of all of these tests; a green square in the pairwise matrix is
 935 indicative of a positive test for the pairwise comparison and thus provides potential
 936 evidence of recombination.

937
 938



939
 940
 941
 942
 943
 944
 945
 946

Figure 5. Genome-wide SNP frequency highlights hotspots. For each panel, the frequency of SNPs in 5-kb windows is shown across the genome. The genome assembly of isolate CBS 11892 was used for all comparisons, and scaffolds are ordered along the x-axis with grey lines representing scaffold boundaries. Red dots indicate the position of the mating type locus.

947 **Supplemental Figure and Table Legends**

948

949 **Figure S1. ITS sequence variation in *T. interdigitale*.** Aligned ITS sequence is shown
950 for four isolates, including the two for which whole genomes were sequenced (H6 and
951 MR816) and two previously characterized isolates (AF168124 and AY062119). Isolate
952 AY062119 has been re-classified as *T. mentagrophytes*. Variant sites are highlighted.

953

954 **Figure S2. Detection of *MAT1-1* in *T. rubrum* and *MAT1-2* in *T. interdigitale* by**
955 **PCR.** A. PCR-based determination of the *MAT1-1* alpha domain of *T. rubrum* isolates:
956 *T. rubrum* MR 851, *T. megninii* CBS 389.58, *T. megninii* CBS 384.64, and *T. megninii*
957 CBS 417.52. The alpha domain *MAT1-1* gene was identified from samples = 1-12 and
958 MR 851 *T. rubrum*; the alpha domain *MAT1-1* gene was not identified from *T. megninii*
959 CBS 389.58, *T. megninii* CBS 384.64, or *T. megninii* CBS 417.52. M: DNA ladder. B.
960 PCR-based determination of *MAT 1-2* HMG domain of *T. rubrum*: *T. rubrum* MR851, *T.*
961 *megninii* CBS 389.58, *T. megninii* CBS 384.64, and *T. megninii* CBS 417.52. The HMG
962 domain *MAT1-2* gene was identified from *T. megninii* CBS 389.58, *T. megninii* CBS
963 384.64, and *T. megninii* CBS 417.52, and was not identified from *T. rubrum* isolate = 1-
964 12 and *T. rubrum* MR 851, M: DNA ladder. C. PCR-based determination of *MAT1-2*
965 HMG domain of *T. interdigitale*. *T. interdigitale* isolates = 1-9, *T. interdigitale* MR8801
966 (positive control), and *T. rubrum* MR851 (negative control), M; DNA ladder. D. PCR
967 based determination of *MAT 1-1* alpha domain of *T. interdigitale* isolates. *T. interdigitale*
968 isolates = 1-9, *T. interdigitale* MR8801 (negative control), and *T. rubrum* MR851
969 (positive control). M: DNA ladder.

970

971 **Figure S3. Phylogenetic relationship and sharing of variant sites of sequenced *T.***
972 ***rubrum* isolates.** A. Phylogenetic relationship of *T. rubrum* isolates inferred using
973 RAxML (Methods). B. Classification of SNP sites based on conservation across the
974 sequenced isolates; unique: only in one isolate; shared: in two to seven isolates; fixed:
975 in all eight isolates.

976 **Figure S4. Lack of decay of linkage disequilibrium (LD) in *T. rubrum*.** LD (r^2) was
977 calculated for all pairs of SNPs separated by 0 to 300 kb and then averaged for every

978 1kb. LD values for each window were then calculated by averaging over all pairwise
979 calculations in the window.

980

981 **Figure S5. Mating assays.** A. Mating assay plate; *T. rubrum* and *T. interdigitale* on E
982 medium. B. Mating assay plate; *T. rubrum* and *A. simii* (a) E medium, (b) Takashio
983 medium eight weeks. C. *T. rubrum* and *T. megninii* on E medium for eight weeks.

984

985 **Figure S6. Read depth of sequenced isolates.** Reads from each isolate were aligned
986 to the *T. rubrum* reference genome and normalized read depth was computed for 5kb
987 windows. Read depth is even across the reference genome for most isolates, with small
988 regions of higher depth detected in some isolates.

989

990 **Figure S7. Variation in LysM-Hce gene cluster across sequenced dermatophytes.**
991 In *T. rubrum*, the LysM-Hce gene is closely linked to two other LysM genes; this
992 organization is most similar to that found in *M. canis*, although these genes are located
993 on two different scaffolds.

994

995 **Table S1. Properties of sequenced isolates.**

996 **Table S2. Accessions for sequenced genomes.**

997 **Table S3. MLST sequence, genotypes, and GenBank accession numbers.**

998 **Table S4. Primers for MLST gene amplification.**

999 **Table S5. *Trichophyton* genome assembly statistics.**

1000 **Table S6. Primer pairs used for mating type determination of *T. rubrum***

1001 **Table S7. Mating assays and results.**

1002 **Table S8. Frequency of SNPs in *T. rubrum* and *T. interdigitale* isolates by mutation
1003 type.**

1004 **Table S9. Duplicated regions in sequence isolates.**

1005 **Table S10. List of genes found in duplicated regions.**

1006 **Table S11. Deleted regions in sequenced isolates.**

1007 **Table S12. List of genes in deleted regions in sequenced isolate**

1008 **Table S13. Genes containing the LysM binding domain in dermatophytes**